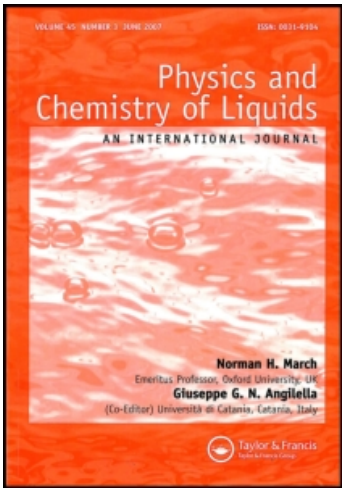

Physics and Chemistry of Liquids
Publication details, including instructions for authors and subscription information:
http://www.informaworld.com/smpp/title~content=t713646857

X-ray Structure Study and Electrical Properties of Some Liquid Cadmium-Zinc Alloys

P. Andonov[a]; A. Bath[b]
[a] Laboratoire de Magnétisme, CNRS 1, Place Aristide, Briand, Meudon, France [b] Laboratoire de Physique des Milieux Condensés Faculté des Sciences, Metz, France

To cite this Article Andonov, P. and Bath, A.(1983) 'X-ray Structure Study and Electrical Properties of Some Liquid Cadmium-Zinc Alloys', Physics and Chemistry of Liquids, 13: 2, 123 — 150
To link to this Article: DOI: 10.1080/00319108308080771
URL: http://dx.doi.org/10.1080/00319108308080771

Phys. Chem. Liq., 1983, Vol. 13, pp. 123–150
0031-9104/83/1302–0123$18.50/0

Printed in Great Britain

X-ray Structure Study and Electrical Properties of Some Liquid Cadmium–Zinc Alloys

P. ANDONOV
Laboratoire de Magnétisme, CNRS 1, Place Aristide Briand 92190 Meudon—France.

and

A. BATH
Laboratoire de Physique des Milieux Condensés Faculté des Sciences, Ile du Saulcy 57000 Metz—France

(*Received May 17, 1983*)

X-ray diffraction patterns of liquid Cadmium–Zinc alloys with 10, 25 and 40 atomic percent Zn were measured. With a focusing diffractometer employing the reflexion geometry and Mo-Kα radiation, the structure factors have been determined in the range of scattering vector $K = 4\pi \sin\theta/\lambda$ between 0.25 $Å^{-1}$ and 17 $Å^{-1}$ at two temperatures 330 and 415°C. Though the alloy near the eutectic composition shows oscillations weakly more apparent than those for the two other compositions, the partial interference functions $J_{ij}(K)$ have been calculated, assuming that they are approximately independent of the atomic concentrations. The reduced partial distribution functions $G_{ij}(r)$ and the probability functions $p_{ij}(r)$ have been evaluated by Fourier transformation of $[J_{ij}(K) - 1]K$. The measured global and partial interference functions are compared with the calculated ones from the hard sphere model. The deviation from the assumption of concentration independence of $J_{ij}(K)$ was evaluated by the variations of the $J(0)$, K_1 and F_F values when they are plotted as a function of concentration ($J(0)$ = asymptotic value of $J(K)$ when $K = 0$; K_1 = position of the first peak maximum of $J(K)$ and K_F = Fermi wave vector). These deviations are not negligible but in the studied range of alloy compositions only small deviations of about 5% are observed.

To examine if the electronic transport properties are sensitive to such a structural effect, thermoelectric power experiments were carried out around the eutectic composition, at different temperatures and just above the liquidus temperature, by using the small ΔT-method. For the resistivity results, we refer to the thorough work of Itami and Shimoji.

Thermopower S and the resistivity ρ_R of the metallic Cd–Zn alloy can be explained by the Faber–Ziman theory. The calculation of S and ρ_R was made by using the volume dependent model potential of Ashcroft and Langreth and as partial interference functions either the hard sphere solution of the Percus–Yevick equation extended to binary alloys or the measured $J_{ij}(K)$.

The theoretical thermopower-concentration and resistivity-concentration isotherms reproduce fairly well the experimental data. The electronic transport properties seem to be poorly affected by slight changes of the structure. This weak influence of the structure is discussed.

1 INTRODUCTION

The electronic transport properties of the Cd–Zn alloys in the liquid state have been studied and show no striking feature versus concentration. The results may be largely explained within the nearly free electron theory of Faber and Ziman.[1] Itami and Shimoji[2] measured the resistivity and compared their data to theoretical calculations. As partial interference functions they used the hard sphere solution of the Percus–Yevick equation extended to binary alloys.[3] For the pseudopotentials they tried successively Ashcroft and Langreth's potential[4] and the more refined Evan's potential.[5] In this way the overall shape of the resistivity-concentration isotherm was obtained. Bath and Kleim[6] measured the thermoelectric power and made use of the substitutional model of Faber and Ziman[1] to explain their results. If one neglects the energy dependence of the potentials, in this model, the thermoelectric power of an alloy is expressed as a function of its resistivity and the resistivities and the thermoelectric powers of the pure components, as shown by Howe and Enderby.[7] Following these lines, only small differences were observed between the theoretical curve and the experimental one.

On the basis of the thermodynamic properties,[8] the hypothesis of the substitutional model are likely to be fulfilled for the Cd–Zn system. This system shows a simple eutectic phase diagram with primary solid solutions where the eutectic temperature is 266 $\pm$ 3°C and the eutectic composition varies between 26–26.8 atomic percent Zn (see the phase diagram of Hansen and Anderko[9]).

The liquid solution is nearly regular. The thermodynamic data of mixing are symmetric about the concentration $c = 0.5$ (Hultgren *et al.*[8]). The enthalpy of mixing ΔH is parabolic with a maximum equal to 2.1 KJ/mole at 803°K ($Nk_BT \simeq 6.6$ JK/mole). In this model the Gibbs free energy of mixing ΔG is given by:

$$\Delta G = c_1 c_2 N\omega + Nk_BT(c_1 \ln c_1 + c_2 \ln c_2) \tag{1}$$

where the second term is just $(-T)$ times the entropy of random mixing of a ideal solution and ω an interchange energy, assumed to be concentration independent. A positive ω implies that like-atom nearest-neighbour pairs are preferred over unlike atom pairs and vice-versa for ω negative (for the ideal solution $\omega = 0$).

The limits of model validity are reported by Bhatia.[10] With the formalism of Bhatia and Thornton,[11] the limit of structure factors of a binary mixture when the wave-length vector $k = 4\pi \sin \theta/\lambda$ tends to zero is determined by the mean square fluctuations in the composition of the alloy, in particular

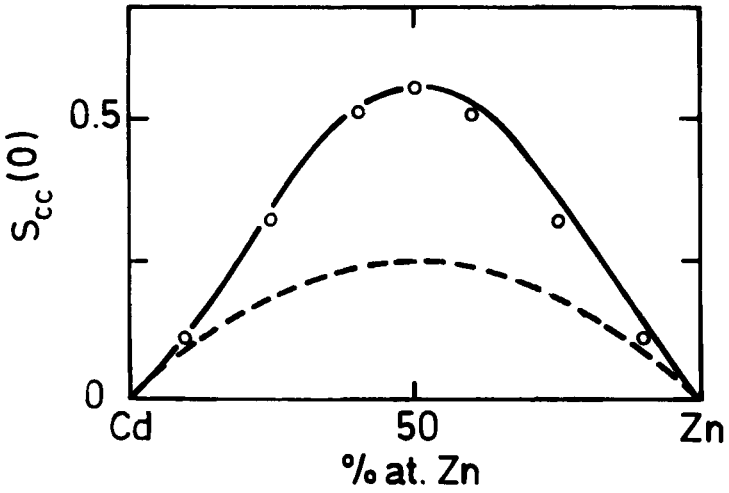

FIGURE 1 $S_{cc}(0) = f(c)$ of Cd–Zn system at 530°C - - - ideal $S_{cc}(0)$ —o—o calculated $S_{cc}(0)$ from Eq. (2) with $w/k_BT = 1.1$.

with the concentration fluctuations

$$S_{cc}(0) = \frac{c_1 c_2}{[1 - (2\omega/k_B T)c_1 c_2]} \tag{2}$$

the curve $S_{cc}(0)$ versus c, deduced from the tabulated data of Hultgren *et al*[8] or from the more recent experimental activity data[12–13] is symmetric about $c = 0.5$. The same behaviour is obtained from the precedent equation when $\omega/k_B T \simeq 1.1$ (See Figure 1). An asymmetry due to a size effect is not observed.

For such a system, it is supposed that the mean atomic volume of the alloys follows the ideal law of mixing. Such an approximation is well supported by the density measurements. The excess volume of mixing measured by Kleppa *et al.*[14] is weakly positive with a maximum at the high Cd concentration ($c \simeq 0.2$ atomic percent Zn) equal to 0.07 cm^3/mole. In the same range of concentration, Ptak and Kucharski[15] have obtained a weakly negative excess volume equal to -0.05 cm^3/mole. With the experimental accuracy both values are possible; the ratio $|V_e|/V_{id}$ remains lower than 0.5% (V_e = excess volume, V_{id} = ideal volume corresponding to linear interpolation of Vegard's law).

But from structural point of view, clearly the hypothesis of the substitutional model are not well satisfied for the Cd–Zn system. The Fermi wave vector K_F varies from 1.36 $Å^{-1}$ for pure cadmium to 1.53 $Å^{-1}$ for pure zinc and further the interference functions of the pure metals should at least be identical, which is not the case[16–18]—(see Figures 3 and 4).

The aim of this work is to get better information about the structure to improve the calculation of the resistivity and the thermoelectric power. X-ray diffraction experiments were performed on three liquid alloys to extract the partial interference functions $J_{ij}(K)$ by the concentration method. This method is only rigorously valid for an ideal mixture where the three partial interference functions are identical. The hypothesis of the invariance of the $J_{ij}(K)$ with composition limits the applicability of the method to the systems which exhibit no important structural modifications versus concentration. Our diffraction measurements showed that for the alloy near the eutectic composition, the oscillations of the total interference function are somewhat more apparent than those for the two compositions.

It is then interesting to look if this feature is of some consequence on the electrical properties; particularly the thermopower should be sensitive to the values of the partial interference functions at 2 K_F. To examine if the electronic transport properties are sensitive to such a weak structural effect, thermoelectric power experiments were carried out around the eutectic composition and just above the liquidus temperature. We refer to the thorough work of Itami and Shimoji[2] for the resistivity results which remain a smooth function versus concentration without particular behaviour

II EVALUATION METHODS OF THE STRUCTURAL AND ELECTRICAL PROPERTIES

A Structure study

α) *partial interference functions* The total interference function in terms of the coherently scattered intensity $I_{eu}^{coh}(K)$ per atom in electron units can be defined by:

$$J(K) = [I_{eu}^{coh}(K) - \langle f^2 \rangle + \langle f \rangle^2]/\langle f \rangle^2 \tag{3}$$

with:

$$I_{eu}^{coh}(K) = \langle f^2 \rangle + \langle f \rangle^2 \int_0^\infty 4\pi r^2[\rho(r) - \rho_0] \frac{\sin Kr}{Kr} \, dr \tag{4}$$

where the mean and mean square scattering factors are:

$$\langle f \rangle = \sum_i c_i f_i \quad \text{and} \quad \langle f^2 \rangle = \sum_i c_i f_i^2$$

c_i being the atomic concentration of the element i, $\rho(r)$ and ρ_0 the weighted and average atomic densities respectively.

The weighted radial density or pair distribution function is given by the expression:

$$\rho(r) = \sum_i \sum_j c_i f_i c_j f_j \rho_{ij}(r)/\langle f \rangle^2 \tag{5}$$

where $\rho_{ij}(r)$ is the number of atoms of type j per unit volume at a distance r from an i-type atom.

For a liquid binary alloy the structure is characterized by the three partial interference functions $J_{ij}(K)$. On neglecting the small angle scattering, these functions are connected with $I_{eu}^{coh}(K)$ by:

$$I_{eu}^{coh}(K) = \langle f^2 \rangle - \langle f \rangle^2 + \sum_i \sum_j c_i c_j f_i f_j J_{ij}(K) \tag{6}$$

Using Eqs. (3) and (6) we can write:

$$J(K) = \sum_i \sum_j c_i c_j f_i f_j J_{ij}(K) / \langle f \rangle^2$$

or

$$J(K) = w_{11} J_{11}(K) + w_{22} J_{22}(K) + 2w_{12} J_{12}(K) \tag{7}$$

The atomic scattering factors are functions of K for X-ray diffraction, the weighting factor is given by:

$$w_{ij} = \{c_i c_j f_i(K) f_j(K)\} / \langle f(K) \rangle^2 \tag{8}$$

In order to determine $J_{ij}(K)$ one needs three total interference functions where the w_{ij} values are different. With assumption of concentration independence of $J_{ij}(K)$, it is enough to measure the scattering intensity from three alloys of different concentrations and then to solve the set of three equations (7) to determine the three partial functions.

The $J_{ij}(K)$ are deduced from the solution of the matrix form

$$[Y(K)] = [A][X(K)]$$

where

$$X = \begin{vmatrix} J_{11} - 1 \\ J_{22} - 1 \\ J_{12} - 1 \end{vmatrix}; \qquad Y = \begin{vmatrix} J_{(c_1, c_2)} - 1 \\ J_{(c_1', c_2')} - 1 \\ J_{(c_1'', c_2'')} - 1 \end{vmatrix}$$

and the determinant $[A]$ given by:

$$\begin{vmatrix} \dfrac{c_1^2 f_1^2(K)}{\{c_1 f_1(K) + c_2 f_2(K)\}^2} & \dfrac{c_2^2 f_2^2(K)}{\{c_1 f_1(K) + c_2 f_2(K)\}^2} & \dfrac{2c_1 c_2 f_1(K) f_2(K)}{\{c_1 f_1(K) + c_2 f_2(K)\}^2} \\ \dfrac{c_1'^2 f_1^2(K)}{\{c_1' f_1(K) + c_2' f_2(K)\}^2} & \dfrac{c_2'^2 f_2^2(K)}{\{c_1' f_1(K) + c_2' f_2(K)\}^2} & \dfrac{2c_1' c_2' f_1(K) f_2(K)}{\{c_1' f_1(K) + c_2' f_2(K)\}^2} \\ \dfrac{c_1''^2 f_1^2(K)}{\{c_1'' f_1(K) + c_2'' f_2(K)\}^2} & \dfrac{c_2''^2 f_2^2(K)}{\{c_1'' f_1(K) + c_2'' f_2(K)\}^2} & \dfrac{2c_1'' c_2'' f_1(K) f_2(K)}{\{c_1'' f_1(K) + c_2'' f_2(K)\}^2} \end{vmatrix}$$

Remark We have seen that the extraction method used in this work, is only rigorously valid for an ideal mixture where the three partial interference

functions are identical. This condition is never fulfilled. To elucidate the physical significance of this method and its validity for the Cd–Zn alloys an analytical solution for the partial function on the basis of the Percus–Yevick equation[3,19–20] is used to calculate the theoretical $J_{ij}(K)$ for the different $(c_i c_j)$ alloys studied in this work. Then the global interference function, reconstructed from the theoretical $J_{ij}(K)$, will be compared with the experimental ones. But a good agreement between such a reconstruction and the experimental curves cannot be considered as the justification of the initial assumption about the concentration independence of $J_{ij}(K)$. It is a necessary but not sufficient condition because the global interference function can be reconstructed, within the experimental accuracy, with a wide variety of $J_{ij}(K)$ functions. The experimental partial functions will be roughly accurate only if these functions depend very slightly on concentration in the interval of the studied compositions. The method validity is verified by the study of the variations of the structure factor characteristics versus concentration:

$$J_{(0)} = f(c); \qquad K_1 = f(c) \text{ and } 2K_F = f(c)$$

$J(0)$ = asymptotic value of $J(K)_{K=0}$; K_1 = position of the first peak maximum.

β Partial distribution functions From the precedent equations the partial interference functions $J_{ij}(K)$ can be expressed by:

$$J_{ij}(k) = 1 + \int_0^\infty 4\pi r^2 \rho_0 \left[\frac{\rho_{ij}(r)}{\rho_j} - 1\right]\{(\sin Kr)/Kr\}\mathrm{d}r \tag{9}$$

with $\rho_j = c_j \rho_0$

The partial radial distribution functions are obtained by Fourier transformation of $J_{ij}(k)$. These functions may be written in terms of:
—reduced distributions:

$$G_{ij}(r) = 4\pi r\left[\frac{\rho_{ij}(r)}{c_j} - \rho_0\right] = \frac{2}{\pi}\int_0^\infty K[J_{ij}(K) - 1]\sin Kr\, \mathrm{d}K \tag{10}$$

—and pair-probability functions:

$$p_{ij}(r) = \rho_{ij}(r)/(c_j\rho_0) = 1 + \frac{1}{2\pi^2\rho_0 r}\int_0^\infty K[J_{ij}(K) - 1]\sin Kr\, \mathrm{d}K \tag{11}$$

Any oscillations of $G_{ij}(r)$ below r_0 (r_0 = hard sphere diameter of the atoms) must be due to errors of evaluation of $J_{ij}(K)$ since $\rho_{ij}(r) = 0$ for $r < r_0$. Therefore $G_{ij}(r) = -4\pi r\rho_0$ in this domain. In the used calculation method, it was assumed that the $J_{ij}(K)$ are independent of concentration, but the value of ρ_0 is not known. In the region $r < r_0$, to follow the procedure of

Kaplow *et al.*[21] we draw an average straight line through all experimental points of $G_{ij}(r)$ and we use these interpolated values to recalculate $J_{ij}(K)$ by Fourier inversion. By this repeated procedure $J_{ij}(K) \rightleftarrows G_{ij}(r)$ we obtain the refined partial functions.

The position r_1 of the first peak maximum of $p_{ij}(r)$ is a measure of the interatomic separation between ij atom pairs. The partial radial distribution functions (P.R.D.F.) allow us to determine the coordination numbers:

$$\eta_{ij} = \int_{r_0}^{r_2} 4\pi r^2 \left\{\frac{\rho_{ij}(r)}{c_j}\right\} \mathrm{d}r \tag{12}$$

where r_0 is the value of r below which the P.R.D.F. is zero and r_2 is the position of the first minimum of the P.R.D.F.

B Electronic transport properties

The electrical resistivity ρ_R and the thermoelectric power S of such alloys can be explained by the Faber–Ziman theory. The resistivity may be written in the form:

$$\rho_R = c_1^2\rho_{R^{11}} + c_2^2\rho_{R^{22}} + 2c_1c_2\rho_{R^{12}} + c_1c_2M\int_0^1 4\Delta u^2x^3\,\mathrm{d}x \tag{13}$$

where

$$\rho_{R_{ij}} = M\int_0^1 4u_iu_jJ_{ij}x^3\,\mathrm{d}x \qquad (i, j = 1 \text{ or } 2)$$

with $M = 3\pi\Omega/\hbar e^2v_F^2$ and $x = K/2K_f$ and $\Delta u = (u_1 - u_2)$.
In the above expressions Ω is the mean atomic volume, v_F the Fermi velocity and $c_1 = 1 - c_2$ is the atomic concentration of component 1 (cadmium); $u_i(i = 1 \text{ or } 2)$ is the pseudopotential of the component i in the alloy, and the J_{ij} are the partial interference functions.

S is given by the usual relation:

$$S = -\{\pi^2k_B^2T/3|e|E_F\}\chi \tag{14}$$

Where k_B is the Boltzmann constant and E_F the Fermi energy. The thermoelectric parameter χ, defined as:

$$\chi = -\left(\frac{\partial \ln \rho_R(E)}{\partial \ln E}\right)_{E=E_F}$$

can be written in the form:

$$= 3 - (1/\rho_R)\{c_1^2(3 - \chi_{11})\rho_{R^{11}} + c_2^2(3 - \chi_{22})\rho_{R^{22}} + 2c_1c_2M[\Delta u^2 + 2u_1u_2J_{12}]_{K=2K_F} + c_1c_2I\}$$

Where:

$$I = (M/4K_F^4)(\alpha + \beta)$$

$$\alpha = K_F \int_0^{2K_F} \Delta u \left\{ \left(\frac{\partial u_1}{\partial K} \right) - \left(\frac{\partial u_2}{\partial K} \right) \right\} K^3 \, dK$$

$$\beta = K_F \int_0^{2K_F} \left\{ (u_1 \left(\frac{\partial u_2}{\partial K} \right) + u_2 \left(\frac{\partial u_1}{\partial K} \right) \right\} J_{12} K^3 \, dK$$

and $\chi_{ii} = 3 - 2q_{ii} - (r_{ii/2})$

With

$$q_{ii} = \frac{\{(u_i^2 J_{ii})_{K=2K_F}\}}{\int_0^1 4u_i^2 J_{ii} x^3 \, dx}$$

and

$$r_{ii} = \frac{K_F \int_0^1 4\{\partial(u_i^2)/\partial K\}_{K=K_F} J_{ii} x^3 \, dx}{\int_0^1 4u_i^2 J_{ii} x^3 \, dx}$$

The calculation of ρ_R and S was made by using the volume dependent model potential of Aschcroft and Langreth[4] and the hard sphere solution of the Percus–Yevick equation,[3] which at least takes account of the size effect. The used values of packing fraction η_i and hard sphere diameters σ_i are given in Table Ia, (for their determination, see paragraph IVa).

The core parameters R_i were determined in such a way that the theoretical resistivity value of the pure metal, calculated with the hard spheres structure factor[22] reproduces the experimental one, either with Hartree screening (ε_H) or with improved Vashishta-Singwi[23] ε_{vs} and Toigo-Woodruff[24] $\varepsilon_{T.W}$ screening.

TABLE Ia

Values of packing fractions η_i, hard sphere diameters σ_i, core parameters R_i and Γ_i used in the calculation of the electronic transport properties.

420°C	Cd		Zn	
η_i	0.445		0.450	
σ_i(Å)	2.718		2.422	
	R_i(Å)	Γ_i	R_i(Å)	Γ_i
ε_H	0.748	0.181	0.694	0.167
$\varepsilon_{V.S.}$	0.725	0.165	0.673	0.155
$\varepsilon_{T.W.}$	0.720	0.155	0.667	0.146

TABLE Ib

The parameters R_i and Γ_i obtained from the experimental structure factors of pure metals (Zn: Knoll,[17] Andonov,[18] Cd: Waseda[30])

420°C	Cd		Zn	
	R_i(Å)	Γ_i	R_i(Å)	Γ_i
ε_H	0.744	0.227	0.685	0.195
$\varepsilon_{V.S.}$	0.721	0.211	0.665	0.178
$\varepsilon_{T.W.}$	0.715	0.199	0.660	0.167

The core parameters and the hard sphere diameters are held constant in the alloys. Moreover it is supposed that the mean atomic volume of the alloys follows the ideal law of mixing.

For the thermopower calculation, we need the energy derivative of the potential. Following the lines of Ashcroft,[25] we take account of this for the pure metals, through an explicit energy dependence of the core parameters. χ may be expressed with a new parameter:

$$\Gamma_i = -\left(\frac{\partial \ln R_i(E)}{\partial \ln E}\right)_{E=E_F} \qquad (i = 1 \text{ or } 2)$$

The parameters Γ_i were calculated so as to reproduce the experimental values of the thermopowers of the pure metals.[6] The energy derivatives $(\partial R_i(E)/\partial E)_{E_F}$ were then held constant for the calculation of the thermopowers of the alloys. The values of the parameters used in the calculation are summarized in Table Ia.

A second set of parameters R_i and Γ_i (Table Ib) was obtained with the use of the measured structure factors of pure Zinc and Cadmium[16–18,30] by using the fitting procedure described above. The differences between the two sets of values arise because the structure factors of these metals do not resemble exactly those for hard spheres.

III EXPERIMENTAL PROCEDURES

A Structure study

Molten cadmium–zinc alloys have been studied by X-ray diffraction, using a focusing diffractometer for liquids.[18] With the Mo–Kα radiation (quartz monocurved crystal monochromator located in the incident beam), the complete diffraction patterns were obtained in the wave vector range $0 < K < 17.5$ Å^{-1}. The high temperature cell reported previously was

closed by a beryllium screen, so the sample is kept at the desired temperature within ± 1°C. A vacuum of 10^{-4} torr is maintained in the camera to avoid oxidation, to minimize air scattering and to obtain a thermal isolation.

The X-ray measurements were carried out through the screen by reflexion on the free upper surface of the liquid for three alloys (90, 75 and 60 atomic percent Cd) and two temperatures (330°C and 420°C). The scattered intensity was counted using a scintillation counter in the step scan mode for a sufficiently large time interval to obtain a statistical error of less than 1 %. In this reflexion geometry, the liquid specimen may be considered infinitely thick, thus the absorption correction is independent of the direction of the incident beam.

After the background was subtracted, the raw intensity data were corrected for polarisation and the Be screen absorption and then converted to absolute intensities expressed in electron units per atom using the high angle normalization procedure.[26] Values given by Sagel[27] and extrapoled to $K = 18$ Å^{-1} were used to account for the Compton scattering. The coherent scattering is estimated with the atomic scattering factors obtained from the analytic expression given by Cromer and Waber[28] corrected for anomalous dispersion by Cromer.[29] The multiple scattering is negligible for the CdZn

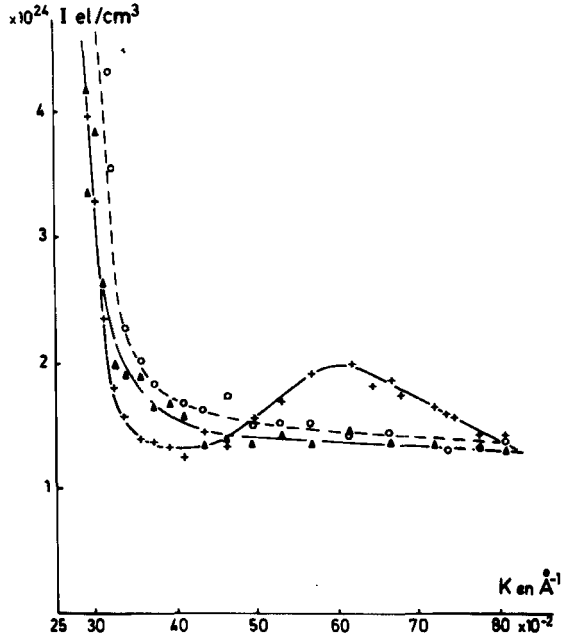

FIGURE 2 Small angle scattering $I = f(K)$ for $Cd_{90}Zn_{10}$ alloy at three temperatures: +:23°C; ▲:400°C and 0 = 460°C.

alloys at high Cd concentration. After the different corrections, the experimental uncertainties lie within 1% for X-ray diffraction. A rapid control of alloys was made using the small angle X-ray scattering. The S.A.S experiments were performed on $Cd_{90}Zn_{10}$ alloy at room temperature and two other temperatures in the liquid state in the range $2.5.10^{-1}$ Å$^{-1} < K < 8.10^{-1}$ Å^{-1} with MoKα radiation. A partial segregation is not observed in the liquid. In Figure 2 the curves corresponding to the liquid state, do not show a maxima like it is observed in the solid state with the high concentration Cd-alloy. The asymptotic value of the scattering intensity, equal to $1.30.10^{24}$ el/cm^3 is in good agreement with the theoretical value of the scattering caused by the atomic fluctuations (calculated value for $Cd_{90}Zn_{10}$ alloy = $1.33.10^{24}$ el/cm^3). The Compton scattering is negligible in the explored range and the weak slope of the two liquid state curves agrees with the secondary scattering of an alloy sample of thickness equal to 20μ.

B Electronic transport properties

The thermoelectric power S was measured for the alloys near the eutectic composition, by using the small ΔT-method. The experimental procedure is essentially the same as that described by Bath and Kleim[31] with slight improvements. Copper alumel couples were used, and copper served as reference material, its absolute thermoelectric power being taken from Cusack[32] (more recent values are published now by Roberts[33]). Including all sources of errors, the absolute uncertainty on the final result should not exceed 0.3 μV.K^{-1}. To test the reproductibility, the two copper alumel couples were replaced by new ones during the study of the eutectic composition (73.5 at.% cadmium). The new experimental points remain in the uncertainty range: see results reported in Figures (9, 10).

IV RESULTS AND DISCUSSION

A Structure study

The experimental interference functions $J(K)$ are reported in Figure 3 for the three Cd–Zn alloys at two temperatures: T_1 = 330°C ($\simeq$40°C and 50°C above the liquidus) and T_2 = 415°C. In this figure, experimentals plots of the pure liquid metals are reported. The previous x-ray data of liquid zinc[18] well agree with the neutron data of Knoll,[17] a very good agreement was found with respect to the position (K_1) and the height $J(K_1)$ of the first peak. For cadmium, the data of North and Wagner[34] show that a change of temperature only has a negligible influence on the K_1 values (2.57 Å^{-1} at 350°C and 2.54 Å^{-1} at 650°C). From our results, the same observation was

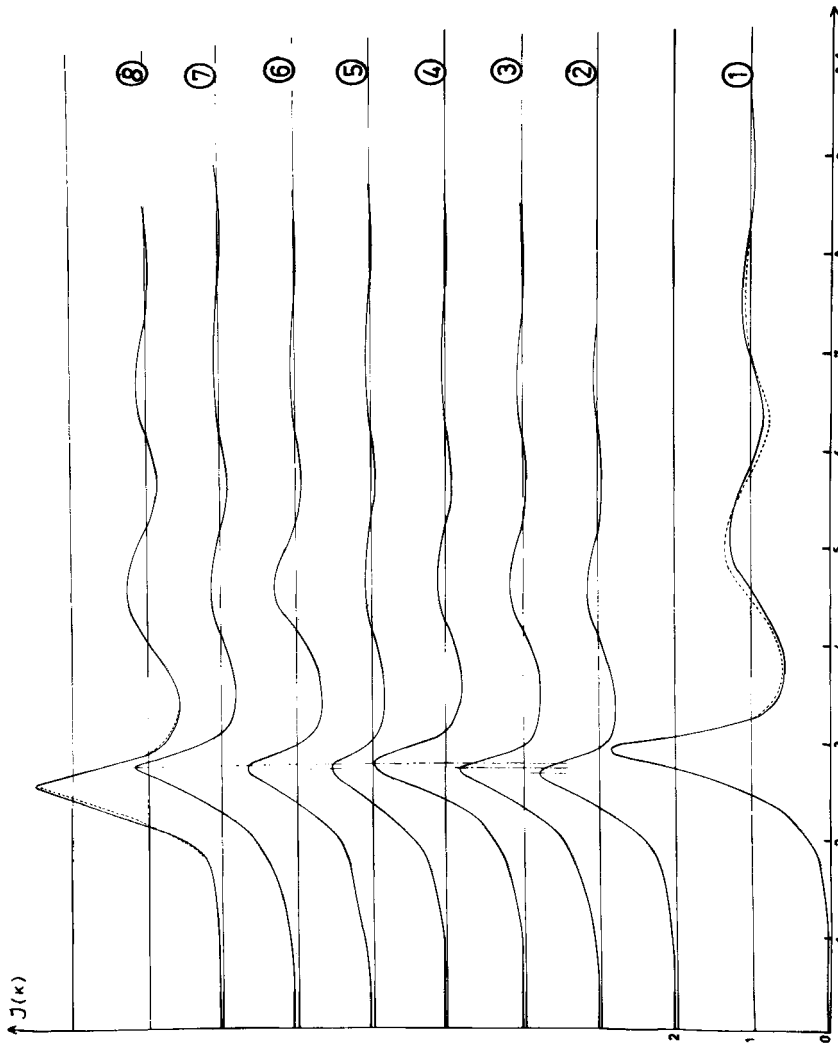

FIGURE 3 Global interference functions 1: liquid zinc: —— 460°C neutron data, Knoll[17]; – – – 550°C X-ray data, Andonov[18]; (2, 3, 4: Cd_{c_1}-Zn_{c_2} alloy at 330°C; 5, 6, 7: Cd_{c_1}-Zn_{c_2} alloy at 415°C) this work, X-ray scattering c_1 and c_2 = 60–40, 75–25 and 90–10 respectively; 8: liquid cadmium – 350°C and . . . 450°C, X-ray data, North and Wagner.[34]

made on the alloys; a variation $\Delta T = 85°C$ does not change perceptibly the K_1 position, so we can use the experimental data obtained at 415°C to calculate the S and ρ_R values and compare them with the experimental electronic transport properties measured at 420°C.

From the three experimental total $J(K)$ curves Figure $3_{5,6,7}$ the experimental partial interference functions are isolated by resolution of the set of Eq. (7). Always, the value of the determinant $|A|$ remains low, so it is very difficult to extract directly the three $J_{ij}(K)$ values.

Let us report the contribution in percent $w_{ij}\%$ of the different pairs of atoms in the Eq. (7) for the three Cd–Zn alloys

		w_{11}	w_{22}	w_{12}
a	$Cd_{90}Zn_{10}$	87,1	0,4	12,5
b	$Cd_{75}Zn_{25}$	67,8	3,1	29,1
c	$Cd_{60}Zn_{40}$	49,0	9,0	42,0

(7)

In 7(a), where the Zn–Zn pairs contribution is negligible, we have considered $J(K)$ only composed of two contributions. In 7(b), the Zn–Zn pairs contribution remains weak, the substitution of the unknown real $J_{22}(K)$ by the calculated one from the Percus–Yevick model applied to the $Cd_{75}Zn_{25}$ alloy [c.$J_{Zn-Zn}(K)$] will produce only a very small error on the Cd–Cd partial interference function ($<0.5\%$). To solve the system of equations, we have extracted the two contributions $J'_{Cd-Cd}(K)$ and $J'_{Cd-Zn}(K)$ from (7a) and (7b) with the previous substitution. A first determination of $J'_{Zn-Zn}(K)$ is obtained from 7(c) where $J'_{Cd-Cd}(K)$ and $J'_{Cd-Zn}(K)$ take the place of the Cd–Cd and Cd–Zn contributions. By a second determination $J''_{Cd-Zn}(K)$ and $J''_{Zn-Zn}(K)$ are extracted from 7(b) and 7(c) where $J'_{Cd-Cd}(K)$ takes the place of the Cd–Cd pairs contribution. Then the different partial functions $J'_{ij}(K)$ and $J''_{ij}(K)$ are fitted to obtain recombinations in good agreement with the global experimental functions (deviations $\leqq \pm 1\%$).

This fitting procedure appears practically unnecessary for $J_{Cd-Zn}(K)$ but it is not negligible for $J_{Zn-Zn}(K)$, particularly in the wave vector range $K < 1$ Å. With this determination the accuracy of the partial interference functions remains similar to the computed ones from the uncertainty on the interference functions through the solution of the matrix form of the system (7). With the low value of the determinant ($|A| = 0.006$ at $K = 0$) and the experimental uncertainties (lie within 1% for X-ray diffraction) the accuracy of the partial interference functions will be only about 5% for J_{Cd-Cd} pairs, 55% for J_{Zn-Zn} pairs and 25% for J_{Cd-Zn} pairs.

The values of $J_{ij}(K)$, in the range of K between 0 and the values of the Fermi wave vector, are of particular interest for the evaluation of the electronic transport properties. The experimental $J_{ij}(K)$ are represented in the limited range $0 < K < 7$ Å^{-1} in Figure $4_{1,2,3}$. A deviation about -10% appears

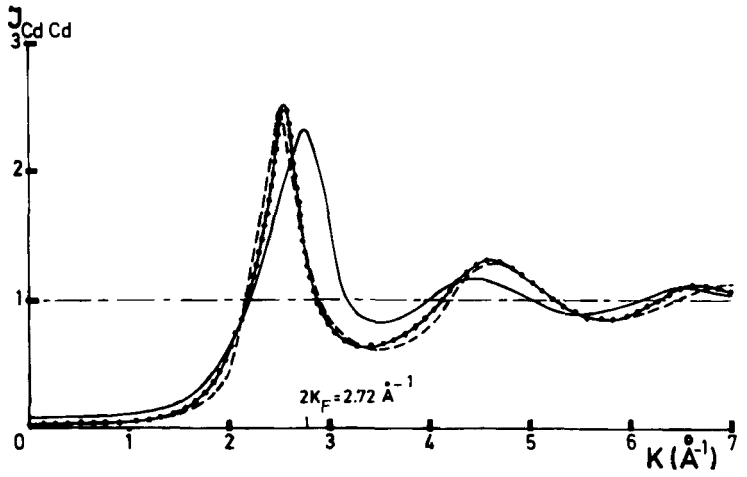

FIGURE 4 Partial interference functions
1) $J_{Cd\text{-}Cd}(K)$ —— experimental curve obtained in this work at 415°C
$J(K)$ •—•—• experimental curve obtained by North and Wagner[34] with pure liquid cadmium at 450°C
$J(K)$ – – – theoretical curve obtained from hard sphere model with $\sigma_{Cd} = 2.72$ Å

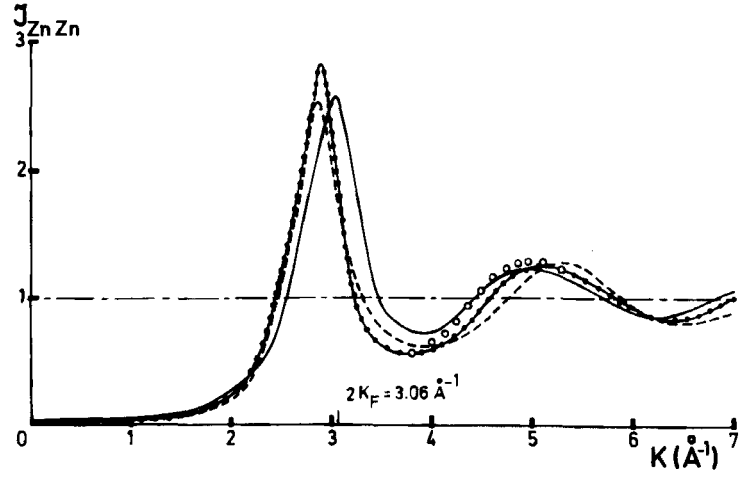

FIGURE 4 Partial interference functions
2) $J_{Zn\text{-}Zn}(K)$ —— experimental curve obtained in this work at 415°C
$J(K)$ •—•—• experimental curve obtained by Knoll[17] with pure liquid zinc at 460°C
○ ○ ○ experimental plot obtained by Andonov[18] with pure liquid zinc at 500°C
$J(K)$ – – – theoretical curve obtained from hard sphere model with $\sigma_{Zn} = 2.42$ Å

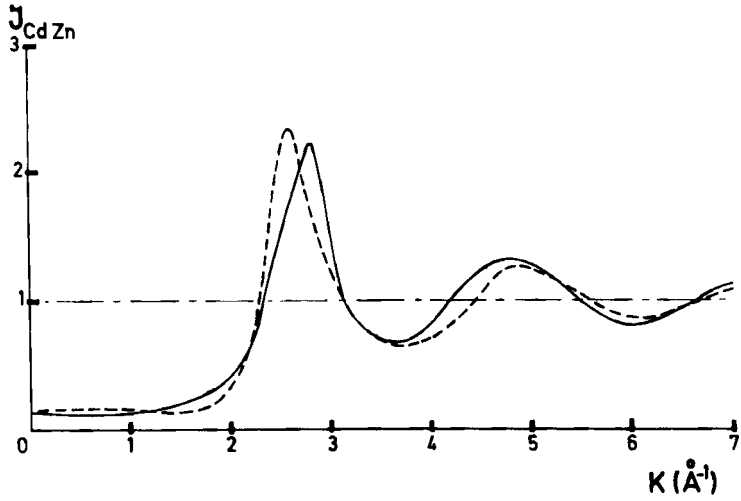

FIGURE 4 Partial interference functions
3) $J_{Cd\text{-}Zn}(K)$ —— experimental curve obtained in this work at 415°C
– – – theoretical curve obtained from hard sphere model with $\sigma_{Cd} = 2.72$ Å, $\sigma_{Zn} = 2.42$ Å and $c_1 = 0.75$,

between experimental and calculated $J_{ij}(K)$ but the most important difference is the shift of K_1 ($\Delta K_1 \simeq +0.10$ Å^{-1}). It should be noted also that the profiles of the first peaks of Zn and Cd are asymmetric and the structure factors of these pure liquid metals are not well described by the hard sphere model.

To calculate $J(K)$ for pure liquid metals, it is necessary to know two of the three variables connected by $\eta = (\pi/6)\rho_0\sigma^3$, with η = packing density; ρ_0 = atomic density and σ = hard sphere diameter we have determined η from two methods:

—the values of the packing density are assumed to be 0.45 at the melting point, at 420°C: $\eta_{Cd} = 0.445$ and $\eta_{Zn} = 0.450$.

—the values of the packing density are obtained from the limit value of $J(K)$ at $K = 0$; with $J(0) = (1 - \eta)^4/(1 + 2\eta)^2$.

$J(0)$ being

—either calculated by the thermodynamic limit $J(0) = k_B T\rho_0 x_T$ where k_B = Boltzmann's constant; T = absolute temperature, χ_T: isothermal compressibility

—or obtained by linear extrapolation to $K = 0$ of the experimental $J(K)$

From the experimental results published in the literature: isothermal compressibility,[35] density[15,36–38] and structure factors,[16–18,30,41] the

variations of η and σ are limited:

$$0.450 < \eta_{Zn} < 0.530 \qquad 2.36\ \text{Å} < \sigma_{Zn} < 2.56\ \text{Å}$$
$$0.443 < \eta_{Cd} < 0.477 \qquad 2.64\ \text{Å} < \sigma_{Cd} < 2.79\ \text{Å}$$

The physical properties of these metals are known with a good accuracy and it is not possible to increase the precedent limits to obtain exactly superposition of experimental and computed data. The best fitting is obtained with the hard diameters $\sigma_{Cd} = 2.72$ Å and $\sigma_{Zn} = 2.42$ Å.

To verify the hypothesis of independent $J_{ij}(K)$ versus concentration, we have calculated the $J_{ij}(K)$ for the studied alloys using the Percus–Yevick approximation generalized to a binary alloy.[3,39] The three theoretical $J_{ij}(K)$ are quite significantly dependent of the composition (see Figure $5_{1,2,3}$) in the domain of small K values. Then the theoretical total structure factors are being reconstructed from the theoretical $J_{ij}(K)$. Theoretical and experimental curves are shown in Figure $6_{1,2,3}$. Whatever the alloy may be, disagreements always appear between the curves: positive shift of K_1, important

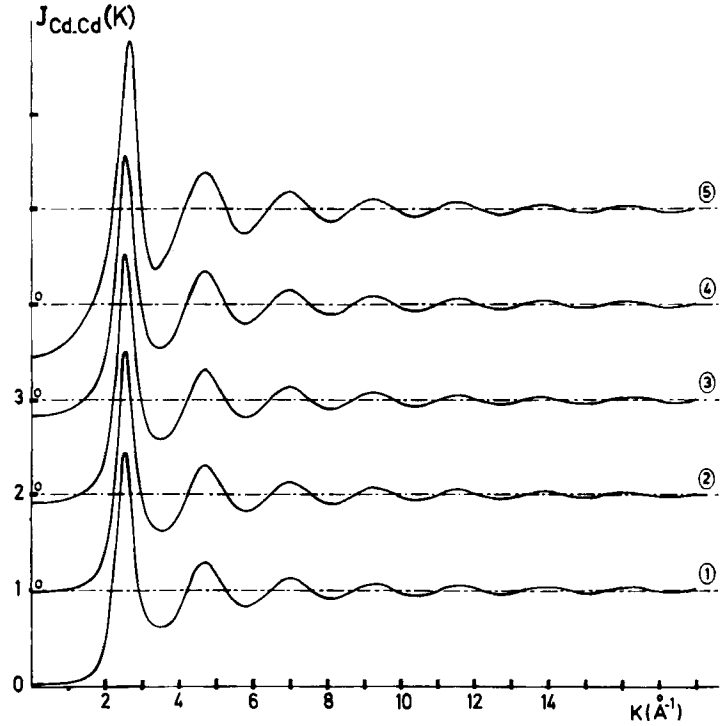

FIGURE 5 $J_{ij}(K)$ calculated from the hard-sphere model
1) $J_{Cd\text{-}Cd}(K)$ 1: pure Cd, 2: $Cd_{90}Zn_{10}$, 3: $Cd_{75}Zn_{25}$
4: $Cd_{60}Zn_{40}$ and 5: Cd_8Zn_{92}

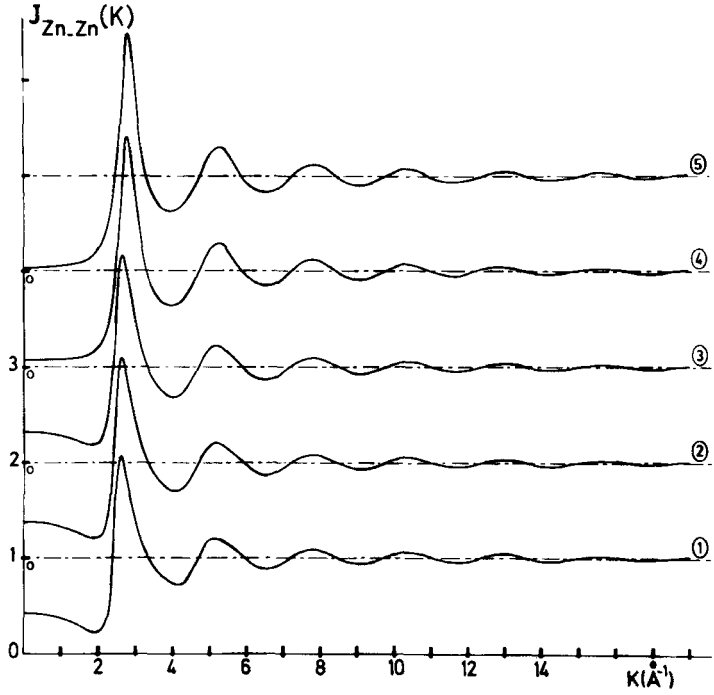

FIGURE 5 $J_{ij}(K)$ calculated from the hard-sphere model
2) $J_{Zn\text{-}Zn}(K)$ 1: $Cd_{90}Zn_{10}$, 2: $Cd_{75}Zn_{25}$, 3: $Cd_{60}Zn_{40}$
4: Cd_8Zn_{92} and 5: pure Zn

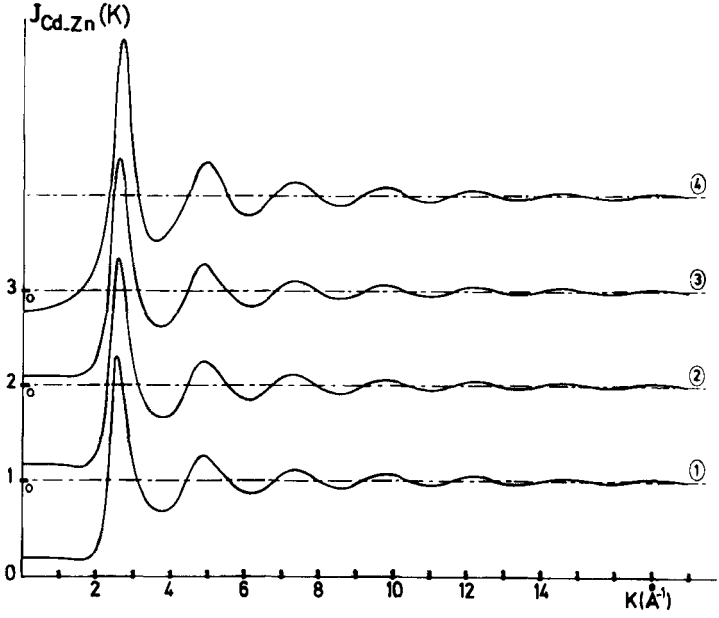

FIGURE 5 $J_{ij}(K)$ calculated from the hard-sphere model
3) $J_{Cd\text{-}Zn}(K)$ 1: $Cd_{90}Zn_{10}$, 2: $Cd_{75}Zn_{25}$, 3: $Cd_{60}Zn_{40}$
and 4: Cd_8Zn_{92}

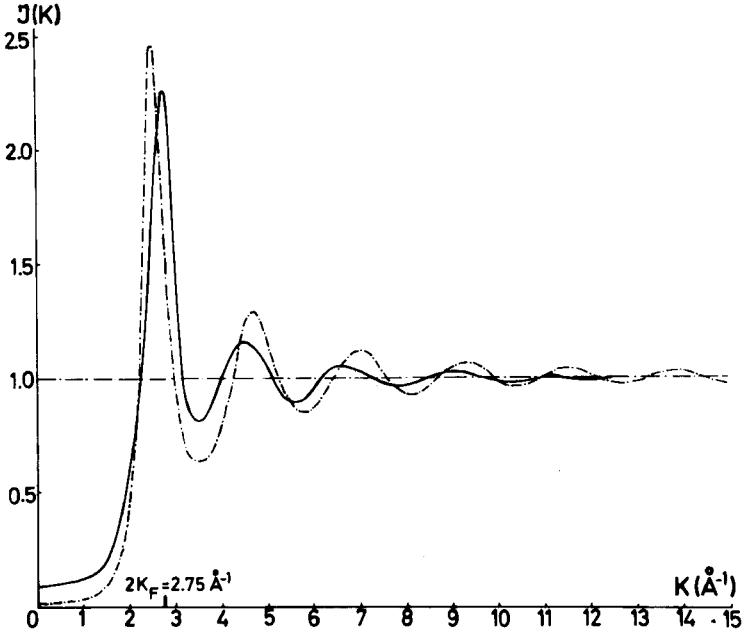

FIGURE 6(1)

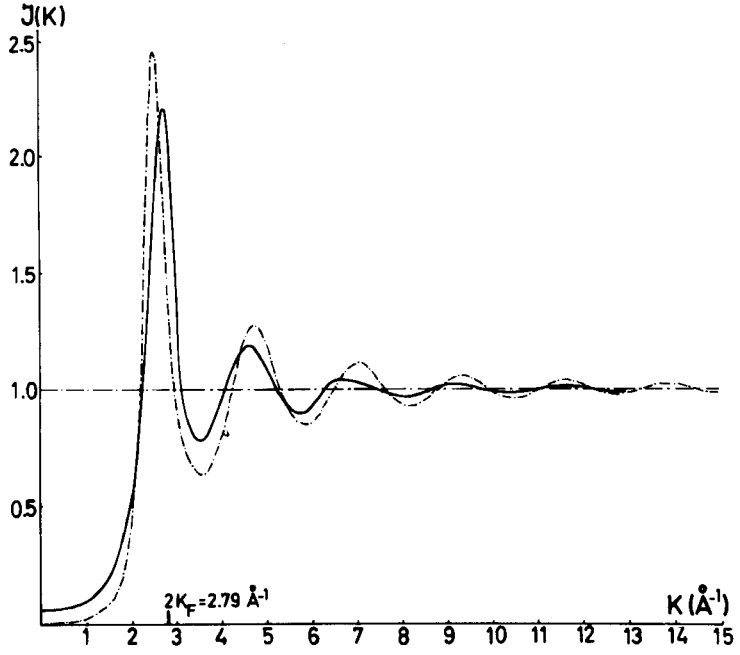

FIGURE 6(2)

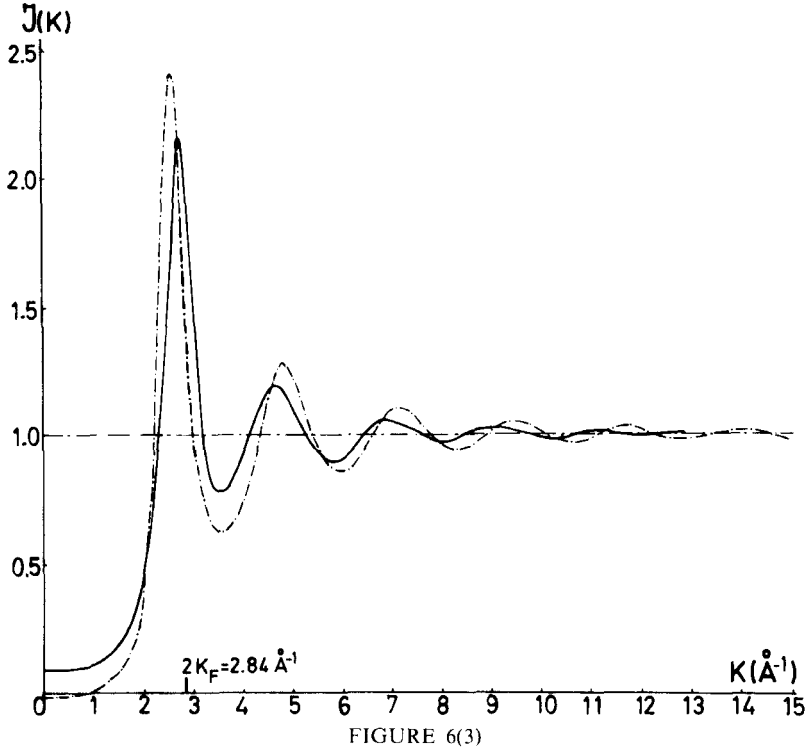

FIGURE 6(3)

FIGURE 6 Total interference functions - - - calculated values, —— experimental values 1) $Cd_{90}Zn_{10}$, 2) $Cd_{75}Zn_{25}$, 3) $Cd_{60}Zn_{40}$

damping of the experimental curves and higher value of total $J(K)$ in the range of $K < 2\ \text{Å}^{-1}$. But these discrepancies do not disprove the previous assumption; to obtain a good validity, it is necessary only that the variations versus concentration remain weak. The variations of K_1, $2K_F$, $J(0)$ and $J_{ij}(0)$ are reported in Figure $7_{1,2}$. Experimental $S(0)$ and K_1 weakly change with concentration. Such trends are also observed for the corresponding theoretical quantities, though the theoretical partials exhibit significant concentration dependence. But this dependence is essentially important at $K = 0$ and decreases for higher values. The total and partial distribution functions are obtained by Fourier transformations of $J(K)$ and $J_{ij}(K)$. The $G_{ij}(r)$ curves are shown in Figure 8. The interatomic distances obtained from the R.D.F. plots and pair probability functions are reported in the Table II with the coordination numbers and those obtained by other authors. The weak variations of atomic density values for the alloys, deduced either from density measurements or from the slope of the average line of $G_{ij}(r)$ in the domain $r < r_0$, support the concentration method.

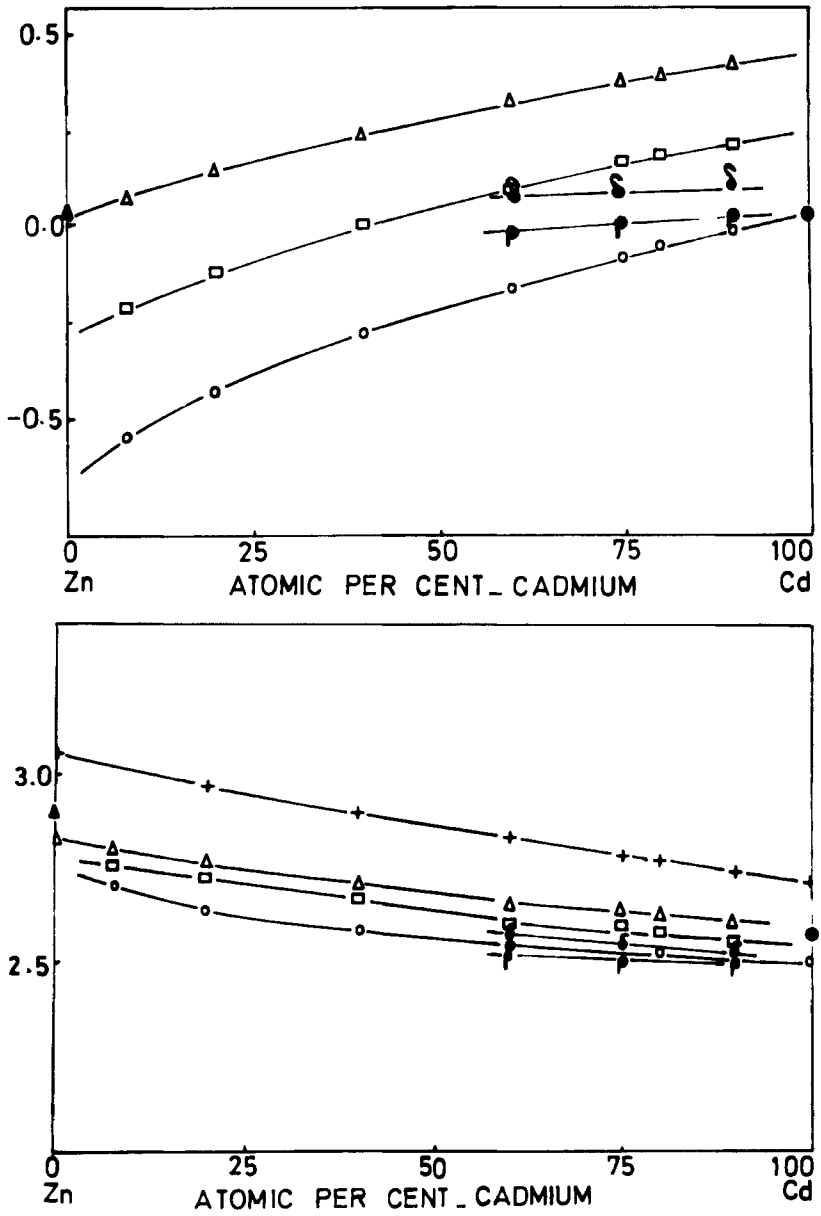

FIGURE 7 Variation of J_0, $J_{ij}(0)$, $2K_F$, K_1 with concentration

7_1: Total $J(\circ)$ and partial $J_{ij}(\circ)$

δ = experimental $J(\circ)$, ρ = theoretical $J(0)$

▲ = experimental pure liquid Zinc △ = theoretical $J_{Zn\text{-}Zn}(0)$

• = experimental pure liquid Cadmium ◦ = theoretical $J_{Cd\text{-}Cd}(0)$

□ = theoretical $J_{Cd\text{-}Zn}(0)$

7_2: $2K_F$ = +

K_1 = δ experimental total function ρ = theoretical total functions

▲ experimental liquid Zinc △ = theoretical partial Zn-Zn

• experimental liquid Cadmium ◦ = theoretical partial Cd-Cd

□ = theoretical partial Cd-Zn

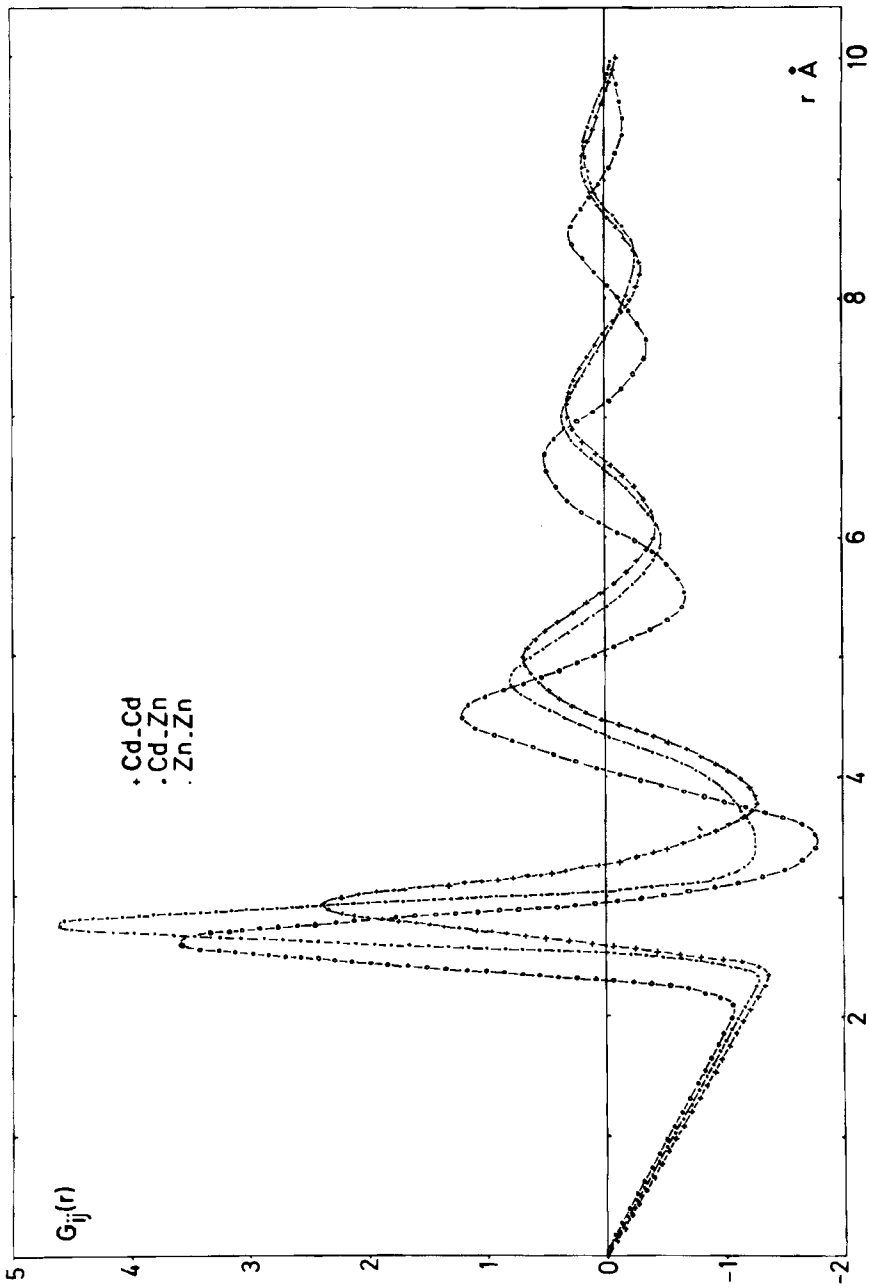

FIGURE 8 Partial radial distribution functions

TABLE II

Interatomic distances and coordinate numbers.

Partial R.D.F.	T°C	r_{1ij} (Å)	r_{2ij} (Å)	n_{1ij} (atoms)	Mean density atom/Å^3	Remarks
Cd-Cd	415	2.96	5.00	8.5	0.04813	In this work ρ_0 is determined by
Cd-Zn	415	2.78	4.80	7.1	0.04559	average straight line through
Zn-Zn	415	2.64	4.50	7.0	0.04306	experimental points of $G_{ij}(r)$ in the region $r < r_0$
Total R.D.F.		r_1	r_2	n_1		
Cd	350	3.11	5.80	10.3	0.04261	Wagner[16]
	420				0.04212	
$Cd_{90}Zn_{10}$	415	2.92	5.30	8.9	0.04376	This work
$Cd_{75}Zn_{25}$	415	2.90	5.27	8.4	0.04563	
$Cd_{60}Zn_{40}$	415	2.87	5.05	8.9	0.04815	
Zn	420				0.06050	
	450	2.68	4.9	10.5		Waseda[30, 41]
	460	2.73 ± 0.02		9.8 ± 0.4	0.06006	Knoll[17]
	458	2.77				
	509	2.79		14.0		Crozier and Seary[42]
	550	2.82 ± 0.05		10.5 ± 0.3	0.05925	Andonov[18]

r_{1ij}: position of the first peak maximum of $G_{ij}(r)$
r_{2ij}: position of the second peak maximum of $G_{ij}(r)$
r_1 : position of the first peak maximum of $G(r)$
r_2 : position of the second peak maximum of $G(r)$
n_{ij} : coordination number obtained from the partial radial distribution functions
n_1 : coordination number obtained from the total radial distribution functions

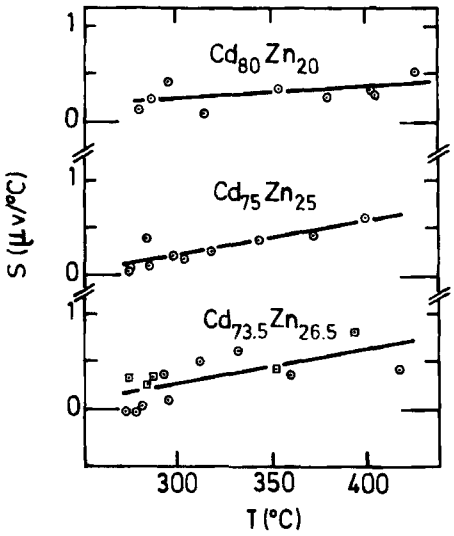

FIGURE 9 Thermoelectric power of cadmium-zinc alloys near the eutectic composition as a function of temperature. ⊙ first thermocouples set ⊡ second thermocouples set.

B Electronic transport properties

The thermoelectric power results are reported in Figure (9). There appeared no anomalous feature just above the liquidus, and the temperature dependence is linear for the three alloys. Further the comparison with the Ref. 6 shows that, within the limits of accuracy, no particular behaviour occurs versus concentration: the thermoelectric power remains essentially a smooth function versus concentration, including the eutectic neighborhood (see Figure 10). Considering the resistivity results of Itami and Shimoji[2] we reach the same conclusion. The resistivity-concentration isotherms are smooth curves. Around the eutectic composition, negative temperature coefficients of the order of -0.01 $\mu\Omega$.cm/°C are found, but pure zinc at the melting point has a temperature coefficient of -0.011 $\mu\Omega$.cm/°C. In the Faber Ziman theory such negative and weakly temperature dependent coefficients may be attributed to the variation of the interference function with temperature when $2K_F$ is nearly equal to K_m [K_m = position of the main peak of the interference function—see e.g. Busch and Güntherodt[40]]. That condition is roughly fulfilled if the mean valency equals 2, which is the case for Cd–Zn system.

The theoretical resistivity-concentration isotherm at 420°C reproduces fairly well the experimental data, as already shown by Itami and Shimoji.[2] For the concentrations $c_1 = 0.8$, 0.735 (eutectic) and 0.7 we obtained

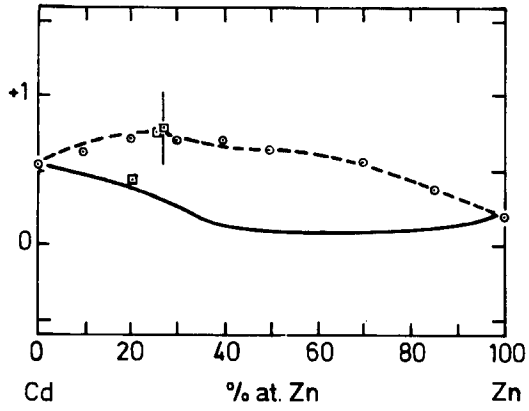

FIGURE 10 Thermoelectric power of cadmium–zinc alloys as a function of composition at 450°C—experimental points ∘ ∞ = Previous results of Bath and Kleim[6] ⊡ = This work—substitutional model of Faber and Ziman[1] ——— = with energy independent potentials – – – = with l chosen as 35 $\mu\Omega \cdot$ cm

respectively with the set of parameters of Table Ia (with $\varepsilon_{T.W.}$) ρ_R = 34.8, 35.1 and 35.2 $\mu\Omega$.cm. The values obtained with ε_H and $\varepsilon_{V.S.}$ are very similar and not reported here.

The calculated thermopower at the same temperature is also weakly composition dependent and for c_1 = 0.8, 0.735 and 0.7 we obtained with $\varepsilon_{T.W.}$, the values $S = -0.05$, -0.16 and -0.20 $\mu V.K^{-1}$. The results differ only slightly from the above values when using ε_H or particularly $\varepsilon_{V.S.}$.

The good agreement achieved for the resistivity shows that no deviation from random packing is needed to explain the experimental data. For the thermoelectric power the deviations remain small (lower than 1 $\mu V.K^{-1}$) nevertheless the calculated values are slightly negative whereas the measured ones are positive.

The next calculation was performed with the partial structure factors deduced from the X-ray diffraction measurements, and with the set of parameters R_i and Γ_i given in Table Ib. The results (with $\varepsilon_{T.W.}$) are reported in Figure 11, and for comparison the calculated ones with hard sphere structure factors (η_i and σ_i of Table Ia) are also given. In Table III the influence of each partial structure factor is indicated by the variations observed between the values obtained with either hard sphere (H.S.) or experimental (exp.) partial structure factors. The results of Figure 11 show that resistivity is less affected by the choice of the partial structure factors than the thermoelectric power. With the experimental structure factors the resistivity concentration isotherm is in good agreement with the experimental data. The calculated thermoelectric power, despite it becomes positive, does not better

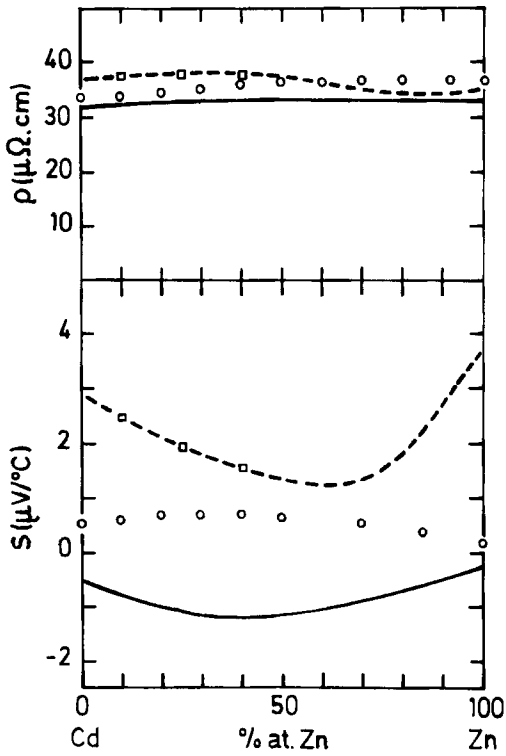

FIGURE 11 Resistivity and thermopower of Cd–Zn alloys versus concentration at 420°C ○ ○ ○ = experimental points. Computation from the model potential of Ashcroft with Toigo-Woodruff screening ($\varepsilon_{T.W.}$) — (R_i and Γ_i of Table Ib). – –⊡– – partial experimental structure factors ——— partial hard sphere model structure factors

TABLE III

Resistivity $\rho_R(\mu\Omega \cdot \text{cm})$ and thermoelectric power $S(\mu V \cdot K^{-1})$ calculated with R_i and Γ_i of Table Ib, with $\varepsilon_{T.W.}$ and the structure factors obtained either from hard spheres model (h.s.) or from experimental results (exp).

P.S.F.			$Cd_{90}Zn_{10}$		$Cd_{75}Zn_{25}$		$Cd_{60}Zn_{40}$	
$a_{Cd\text{-}Cd}$	$a_{Cd\text{-}Zn}$	$a_{Zn\text{-}Zn}$	ρ	S	ρ	S	ρ	S
h.s.	h.s.	h.s.	32.30	– 0.81	32.88	– 1.09	33.16	– 1.18
exp.	h.s.	h.s.	38.00	2.04	38.59	0.97	37.87	0.13
h.s.	exp.	h.s.	31.98	– 0.41	33.30	– 0.21	35.08	– 0.09
h.s.	h.s.	exp.	32.10	– 0.77	31.82	– 0.89	31.01	– 0.68
exp.	exp.	exp.	37.47	2.45	37.94	1.93	37.65	1.56

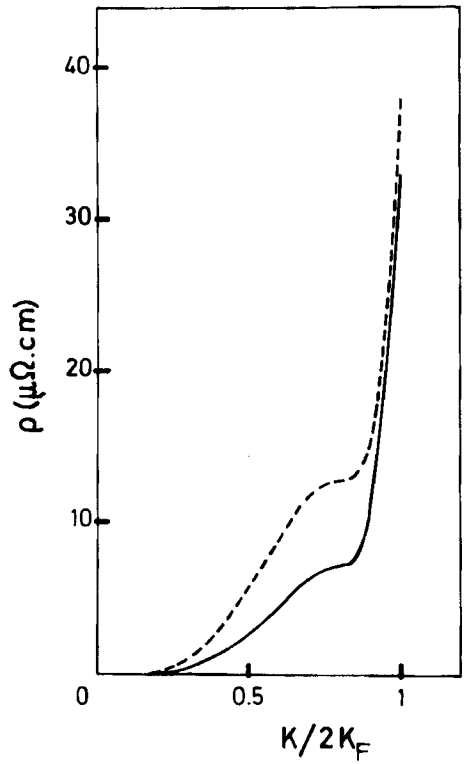

FIGURE 12 Evolution of the theoretical $\rho_R(x)$ versus x for $Cd_{75}Zn_{25}$ alloy at 420°C —— computed values from hard sphere model $J_{ij}(K)$ - - - computed values from experimental $J_{ij}(K)$.

reproduce the measured concentration dependence than the theoretical hard sphere result.

The evaluation of the resistivity (see Eq. (13)) involves integration of partial structure factors (P.S.F.) and model potentials, weighted by x^3 for x varying from 0 to 1. In Figure 12 the evolution of $\rho_R(x)$ is reported with either theoretical or experimental P.S.F., the resistivity being $\rho_R(1)$. As shown earlier, the deviations between these two sets of P.S.F. are important only for small x values. Modulated by x^3, the differences between the P.S.F. have thus weak influence on the resistivity. The thermoelectric power is more sensitive to slight changes of the P.S.F. because it also depends on their particular values at $K = 2K_F$ (see formula (14)).

V CONCLUSION

A structure investigation by X-ray diffraction has been performed on three Cd–Zn alloys. The sample near the eutectic composition seems to present some more structure. The three partial structure factors obtained by the "concentration method" are used to calculate the electrical properties. We found that the appliance of a disordered structure, through the hard sphere model, in the Faber–Ziman theory, leads to an overall good agreement, despite the use of a simple model potential. The use of the experimental P.S.F. does not improve significantly the results. From our structural data we presumed that some effects may occur on the electrical properties around the eutectic composition. But the resistivity, which essentially involves integration of the interference functions up to $2K_F$ with appropriate potentials and weighting factors, seems to be only poorly affected by slight changes of the structure. The thermopower, which was expected to be more structure sensitive, through its dependence of the values of $J_{ij}(K)$ at $2K_F$, exhibits no significant modification too, versus concentration.

Acknowledgements

The X-ray experiments were performed at the "Laboratoire de Physique des Solides" of Orsay University and the electrical properties measurements at the "Laboratoire de Physique des Milieux Condensés" of Metz University. The authors would like to thank Professor A. Guinier and Professor R. Kleim for valuable discussions.

References

1. T. E. Faber and J. M. Ziman, *Phil. Mag.*, **11**, 153 (1965).
2. T. Itami and M. Shimoji, *Phil. Mag.*, **25**, 1361 (1972).
3. N. W. Ashcroft and D. C. Langreth, *Phys. Rev.*, **156**, 685 (1967).
4. N. W. Ashcroft and D. C. Langreth, *Phys. Rev.*, **159**, 500 (1967).
5. R. Evans, *J. Phys. C, Metal Phys. Suppl.*, **2**; S 137 (1970).
6. A. Bath and R. Kleim, *Solid State Commun.*, **20**, 365 (1976).
7. R. A. Howe and J. E. Enderby, *Phil. Mag.*, **16**, 467 (1967).
8. R. Hultgren, P. D. Desai, D. T. Hawkins, M. Gleiser, and K. K. Kelley, Selected values of the thermodynamic properties of binary alloys, (Am. Soc. Metals, Metal Park Ohio 1973).
9. M. Hansen and K. Anderko, *Constitution of Binary Alloys*—Second Edition, p. 446–488. McGraw-Hill Book Company, Inc., New York 1958.
10. A. B. Bhatia, Liquid Metals 1976, (*Inst. Phys. Conf. Series* **30**) 21, 1977.
11. A. B. Bhatia and D. E. Thornton, *Phys. Rev.*, **B2**, 3004–3012 (1970).
12. S. Nakazawa, A. Yazawa, and K. Taniuchi, *J. Japan Inst. Met.*, **40**, 526 (1976).
13. S. Ban-Ya, N. Maruyana, *J. Japan Inst. Met.*, **42**, 80 (1978).
14. D. J. Kleppa, M. Kaplan, and C. E. Thalmayer, *J. Phys. Chem.*, **65**, 843 (1961).
15. W. Ptak and M. Kucharski, *Arch. Hutn.*, **19**, 71 (1974).
16. C. N. J. Wagner, *Phys. Letters Vol.*, **30A**, n° 8, 440 (1969). Liquid Metals 1976—(*Inst. Phys. Conf. Ser.*, **30**), 110 (1977).
17. W. Knoll, Liquid Metals 1976: (*Inst. Phys. Conf. Ser.*, **30**), 117 (1977).
18. P. Andonov, *Rev. Phys. Appl.*, **9**, 907 (1974).

19. V. I. Korsunski and Yu. I. Naberukhin, *Phys. Chem. Liq.*, **5**, 137 (1976).
20. J. E. Enderby and D. M. North, *Phys. Chem. Liquids*, **1**, 1 (1968).
21. R. Kaplow, S. L. Strong, and B. L. Averbach, *Phys. Rev.*, **138**, A 1336 (1965).
22. N. W. Ashcroft and J. Lekner, *Phys. Rev.*, **145**, 83 (1966).
23. P. Vashishta and K. S. Singwi, *Phys. Rev.*, **6**, 875 (1972).
24. F. Toigo and T. O. Woodruff, *Phys. Rev.*, **2**, 3958 (1970).
25. N. W. Ashcroft, *J. Phys. C (Proc. Phys. Soc.)*, **1**, 232 (1968).
26. N. S. Gingrich, *Rev. Mod. Phys.*, **15**, 90 (1943).
27. K. Sagel, *Tabellen zur Röntgenstruktur Analyse*, (Springer Verlag, Berlin 1958).
28. D. T. Cromer and J. T. Waber, *Acta Cryst.*, **18**, 104 (1965).
29. D. T. Cromer, *Acta Cryst.*, **18**, 17 (1965).
30. Y. Waseda, Liquid Metals (*Inst. Phys. Conf. Series*, **30**), 230 (1977).
31. A. Bath and R. Kleim, *Rev. Phys. Appl.*, **14**, 595 (1979).
32. N. E. Cusack, *Rep. Prog. Phys.*, **26**, 361 (1963).
33. R. B. Roberts, *Phil. Mag.*, **B43**, 1125 (1981).
34. D. M. North and C. N. J. Wagner, *Phys. Letters*, **30A**, 440 (1969).
35. D. P. Almond and S. Blairs, *J. Chem. Thermodynamics*, **12**, 1105 (1980).
36. L. Dim, A. Bath, J. G. Gasser, J. L. Bretonnet, and R. Kleim, *Phys. Lett. A*, **84A**, 375 (1981).
37. G. M. B. Webber, R. W. B. Stephens, *Physical Acoustics*, **IV**, Part B, Chapter 11 (Academic Press, New York, 1968).
38. O. Kubaschewski, E. L. Evans, and C. B. Alcock, *Metallurgical Thermochemistry* (Pergamon Press, Oxford, 1967).
39. J. L. Lebowitz, *Phys. Rev.*, **133A**, 895 (1964).
40. G. Busch and H. J. Güntherodt, *Solid State Phys.*, **29**, 235 (1974).
41. Y. Waseda, *The Structure of Non Crystalline Materials*, McGraw-Hill, New York, NY (1980).
42. E. D. Crozier and A. J. Seary—*Can. J. Phys.*, **58**, 1338–1399 (1980).